Chinese Chemical Letters 36 (2025) 110128

Contents lists available at ScienceDirect

Chinese Chemical Letters

journal homepage: www.elsevier.com/locate/cclet

Direct observation of natural products bound to protein based on UHPLC-ESI-MS combined with molecular dynamics simulation

Jinqi Yang[a,b], Xiaoxiang Hu[a,b], Yuanyuan Zhang[a,b], Lingyu Zhao[a,b], Chunlin Yue[a,b], Yuan Cao[a,b], Yangyang Zhang[a], Zhenwen Zhao[a,b,*]

[a] Beijing National Laboratory for Molecular Sciences, CAS Research/Education Center for Excellence in Molecular Sciences, Beijing Mass Spectrum Center, Institute of Chemistry Chinese Academy of Sciences, Beijing 100190, China
[b] Graduate School, University of Chinese Academy of Sciences, Beijing 100049, China

ARTICLE INFO

Article history:
Received 19 March 2024
Revised 12 June 2024
Accepted 14 June 2024
Available online 14 June 2024

Keywords:
Natural products (NPS)
Ligands screening
Mass spectrum (MS)
Molecular dynamic simulation (MDS)
Post-column modification
Amyloid β-peptide 42 ($A\beta_{1-42}$)
Green tea

ABSTRACT

The bioactive constituents found in natural products (NPs) are crucial in protein-ligand interactions and drug discovery. However, it is difficult to identify ligand molecules from complex NPs that specifically bind to target protein, which often requires time-consuming and labor-intensive processes such as isolation and enrichment. To address this issue, in this study we developed a method that combines ultra-high performance liquid chromatography-electrospray ionization-mass spectrometry (UHPLC-ESI-MS) with molecular dynamics (MD) simulation to identify and observe, rapidly and efficiently, the bioactive components in NPs that bind to specific protein target. In this method, a specific protein target was introduced online using a three-way valve to form a protein-ligand complex. The complex was then detected in real time using high-resolution MS to identify potential ligands. Based on our method, only 10 molecules from green tea (a representative natural product), including the commonly reported epigallocatechin gallate (EGCG) and epicatechin gallate (ECG), as well as the previously unreported eepicatechin ($4\beta\rightarrow8$)-epigallocatechin 3-*O*-gallate (EC-EGCG) and eepiafzelechin 3-*O*-gallate-($4\beta\rightarrow8$)-epigallocatechin 3-*O*-gallate (EFG-EGCG), were screened out, which could form complexes with $A\beta_{1-42}$ (a representative protein target), and could be potential ligands of $A\beta_{1-42}$. Among of them, EC-EGCG demonstrated the highest binding free energy with $A\beta_{1-42}$ (-68.54 ± 3.82 kcal/mol). On the other side, even though the caffeine had the highest signal among green tea extracts, it was not observed to form a complex with $A\beta_{1-42}$. Compared to other methods such as affinity selection mass spectrometry (ASMS) and native MS, our method is easy to operate and interpret the data. Undoubtedly, it provides a new methodology for potential drug discovery in NPs, and will accelerate the research on screening ligands for specific proteins from complex NPs.

The bioactive constituents in natural products (NPs) have played a crucial role in the field of medicine. Many drugs are either derived or synthesized from them, such as artemisinin and paclitaxel [1,2]. These bioactive constituents can act as protein ligands, regulating cellular signal transduction, enzyme activity, as well as human emotions and related behaviors [3-5]. Therefore NPs serve as an important source of protein ligands, making them valuable in studying protein-ligand interactions and drug discovery.

The traditional approach for screening bioactive constituents from NPs usually involves isolation and enrichment processes, which is time-consuming, sample-consuming, labor-intensive, and inefficient. In recent years, advancements in analytical techniques have allowed for direct identification of bioactive constituents from NPs bound to proteins. One promising technique is affinity selection mass spectrometry (ASMS) [6-8]. This method involves the use of affinity chromatography to enrich protein-small molecule complexes. The enriched complexes are then analyzed using liquid chromatography-electrospray-mass spectrometry (LC-ESI-MS) to detect and identify the dissociated small molecules. ASMS eliminates the need for extraction and isolation, making it a faster and more efficient approach. However, the immobilization of the target protein in ASMS can be time-consuming and may introduce artifacts or alter the native conformation of the protein, potentially leading to false positive or false negative results. Another approach is native mass spectrometry (native MS), which directly detects protein-ligand complexes using nano-ESI MS. The bioactive components are identified from the product ions of the complexes

* Corresponding author.
E-mail address: zhenwenzhao@iccas.ac.cn (Z. Zhao).

https://doi.org/10.1016/j.cclet.2024.110128
1001-8417/

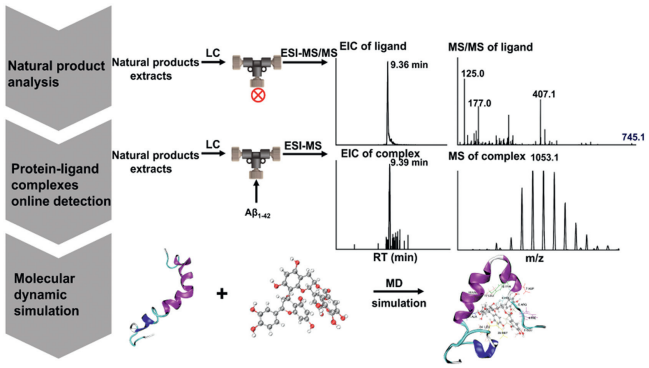

Fig. 1. The workflow for identification of potential ligands from complex NPs bound to a specific protein target based on UHPLC-ESI-MS and MD simulation.

through multi-stage MS [9,10]. Native MS offers the advantage of directly analyzing protein-ligand interactions without the need for the immobilization of the target protein. However, when the NPs sample is complex, the data generated by native MS can be highly complex, making interpretation and analysis challenging. Additionally, competition between bioactive components bound to protein can suppress signals from low abundance or weakly bound components, potentially leading to the loss of important information. To address these challenges, the development of novel, target-based platforms for the rapid screening of NPs bioactive constituents is urgently needed. These platforms should aim to overcome the limitations of these approaches by providing faster, more efficient, and more accurate methods for identifying bioactive components.

In this study, we introduce a novel method combining ultra-high performance liquid chromatography-electrospray ionization-mass spectrometry (UHPLC-ESI-MS) with molecular dynamics (MD) simulation to directly identify NPs bound to specific protein targets. Fig. 1 illustrates the workflow of our approach. The method involves introducing a specific protein target through a three-way valve online, where it forms complexes with NPs components separated by UHPLC. Subsequently, these complexes are detected in real-time using high-resolution MS, facilitating the identification of potential ligands. As a proof-of-concept, we chose amyloid β-peptide 42 ($A\beta_{1-42}$) as a representative protein target and sought its ligands from green tea as a representative natural product. This direct identification of NPs bound to target proteins overcomes the limitations of traditional methods such as ASMS and native MS, thereby facilitating the discovery of potential ligands for specific protein targets and advancing drug development.

Compared to the ASMS method, our approach does not require the immobilization of the target protein, preserving its spatial conformation and reducing the risk of false positives and negatives. In contrast to the native MS method, our strategy separates complex NPs using UHPLC before their interaction with the target protein, reducing competition between bioactive components in NPs and the target protein. This allows even low-concentration bioactive components to form complexes with the target protein, yielding more comprehensive information on protein-NPs ligand interactions. Additionally, data interpretation is simpler compared to native MS, requiring only a comparison of retention time and complex molecular weight information to obtain information on bioactive natural products. Moreover, MD simulation provides valuable insights into the interaction between NPs and the protein target. As a proof-of-concept, we applied this strategy to identify ligands for $A\beta_{1-42}$ from green tea, and in the following sections, we will provide a detailed explanation of its application.

Research has shown that some components in green tea, such as catechins and caffeine, have antioxidant and anti-inflammatory effects, which can provide certain protection against the occurrence and development of Alzheimer's disease (AD) [11]. In addition, the components in green tea can inhibit the pathological processes of AD, such as inhibiting the aggregation and deposition of amyloid β, reducing the formation of neurofibrillary tangles, and improving synaptic function [12]. Therefore, we have chosen green tea as a representative natural product to screen for ligands of amyloid β. First, chromatographic and mass spectrometric conditions were optimized for the analysis of green tea extracts, and the components showed good mass spectrometric signal response in negative ion detection mode. The representative total ion chromatograms (Figs. S1a and b) and corresponding mass spectra (Figs. S1c and d) of the green tea extracts were shown in Fig. S1 (Supporting information). Based on the molecular ion information of the components and the fragment ion information provided by the MS/MS spectra, qualitative analysis of the sample components was performed by combining literature and online database search (HMDB and Massbank) [13-17], and 63 components including 18 catechins, 13 flavonoid glycosides, 11 amino acids, 7 flavonoids, 6 phenolic acids, 2 alkaloids, 2 theaflavins and 4 other kinds of molecules, were identified, as shown in Table S1 (Supporting information).

Among these compounds, catechin dimers were little reported, likely due to the low content and the difficulty of synthesis. Two compounds (theasinensin A (TSA) and epicatechin (4$\beta\rightarrow$8)-epigallocatechin 3-*O*-gallate (EC-EGCG)) were selected from the dimeric catechins as examples for elucidation of structure confirmation. The information of exact masses, MS/MS spectra and possible fragmentation pathways from literature reported was combined for identification [18,19]. The *m/z* values for TSA and EC-EGCG were 914.1525 and 746.1484, respectively. Moreover, by using Xcalibur 3.0 software based on high-resolution mass data, the most probable molecular formula for TSA was calculated to be $C_{44}H_{34}O_{22}$ (with a mass error of 1.81 ppm), and for EC-EGCG was $C_{37}H_{30}O_{17}$ (with a mass error of 0.16 ppm). In addition, Figs. S2a and b (Supporting information) illustrated the MS/MS spectra and fragmentation pathways of TSA and EC-EGCG. Fragment ions of TSA at *m/z* 573.1045 and 591.1145 further generated ions at *m/z* 453.0845 and 465.0826, corresponding to the product of the retro-Diels-Alder reaction (R.D.A reaction) with disrupting one of the oxohexane rings. And the characteristic product ions at *m/z* 425.0866, 423.0716 and 441.0822 generated by R.D.A reaction of EC-EGCG were detected. In this way, TSA and EC-EGCG were identified. Through the above strategies, we identified the main components of crude extracts of green tea, and based on these 63 components in the crude extracts, we further conducted research to screen ligands bound to $A\beta_{1-42}$.

The pathology of AD is characterized by the accumulation of extracellular amyloid-β ($A\beta$) senile plaques and intracellular neurofibrillary tangles of Tau proteins [20]. $A\beta$ is produced by sequential cleavage of the amyloid precursor protein by β- and γ-secretase, and the length of which is variable from 39 to 43 residues [21]. Among them, Aβ1-42 has the highest cytotoxic and aggregation propensity. Pro-fibrillation of $A\beta$ involves the formation of neurotoxic soluble oligomers, protofibrils and amyloid protofibrils [22,23]. Currently for the treatment of AD, scientists have carried out a lot of research on inhibitors targeting $A\beta$ aggregation as well as depolymerization or re-modelling of amyloid fibrils, by using antibodies, nanoparticles and small molecules, etc. [24–29]. Therefore, Aβ1-42 was chosen to seek its ligands from green tea.

The $A\beta_{1-42}$ was injected into the three-way valve through a peristaltic pump and mixed with the outflow of the chromatographic fraction. The green tea extracts flowing out at each moment in the three-way valve had the chance to form a non-covalent complex with $A\beta_{1-42}$ in real time. The formed protein-

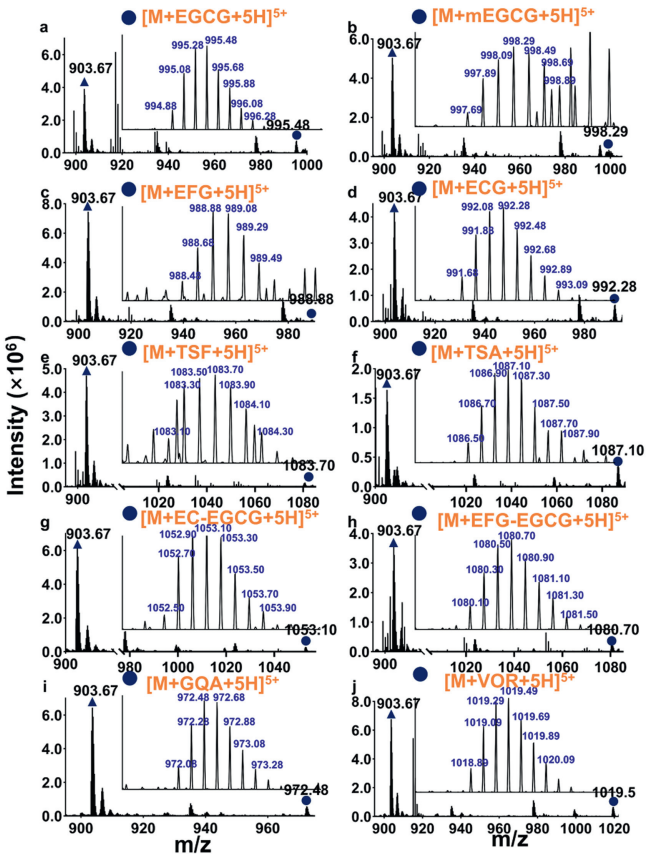

Fig. 2. Mass spectra of the complexes (signals for Aβ_{1-42} were labelled with triangles, and signals for complexes were labelled with circles). (a–j) The complexes formed by Aβ_{1-42} with EGCG, mEGCG, EFG, ECG, TSF, TSA, EC-EGCG, EFG-EGCG, GQA and VOR are shown from a to j, respectively.

ligand complex entered the mass spectrometer ionization source from the other end of the three-way valve and then was detected by MS. The masses of ligands could be calculated by the difference between the masses of the complexes and the masses of the Aβ_{1-42}. By searching the same mass in Table S1, and confirming the same retention time as the complex, the molecule could be identified as ligand molecule.

Taking the EC-EGCG as an example (Fig. 1a and Fig. 2g) for the explanation, a mass signal of the Aβ_{1-42}-ligand complex ($[M+746+5H]^{5+}$) was found at 9.39 min in the extracted ion chromatogram (EIC). In addition to the 5-charged ion signal, the signals of 4-charge (*m/z*: 1316.12) and 6-charge (*m/z*: 875.25) complex ions were also found. Within this retention time, we found a mass peak of 745, corresponding to $[M_{EC-EGCG}-H]^-$ from the EIC of green tea extracts. Therefore, this complex could be deduced to Aβ_{1-42}-EC-EGCG, and EC-EGCC could be a potential ligand bound to Aβ_{1-42}. Eventually we screened 10 molecules from the green tea extracts that could form complexes with Aβ_{1-42}. Figs. 2a–j showed the mass spectra of 10 complexes with the 5-charged adduct ions, and the 10 potential ligands bound to Aβ_{1-42} were listed in Table 1, which containing 4 catechins (epigallocatechin gallate (EGCG), epigallocatechin 3-(3-methyl-gallate) (mEGCG), epicatechin gallate (ECG) and epiafzelechin 3-gallate (EFG)), 4 dimers of catechins epicatechin (4$\beta\rightarrow$8)-epigallocatechin 3-*O*-gallate (EC-EGCG), theasinensin A (TSA), (theasinensin F (TSF) and epiafzelechin 3-*O*-gallate-(4$\beta\rightarrow$8)-epigallocatechin 3-*O*-gallate (EFG-EGCG)) and 2 kinds of other polyphenol (galloylquinic acid (GQA) and vitexin-2′′-*O*-rhamnoside (VOR)).

The effect of incubation duration on forming Aβ_{1-42} protein-ligand was explored. By comparing the mass spectra signals detected immediately or 6 h after mixing Aβ_{1-42} and EGCG, we found that the signal intensity of the complex was almost the same (Fig. S3 in Supporting information), indicating that the incubation time had little effect on the binding. Based on this fact, the method for rapid screening Aβ_{1-42} ligands through post-column modification technology (with a three-way valve to introduce specific protein target) was credible and effective. In addition, if small molecules took a long time to form complexes, the binding affinity was theoretically not expected to be strong, and therefore these protein ligands screened in this way may not be valuable.

The 10 potential ligand molecules we screened were all polyphenolic compounds, and their structures were shown in Table 1. EGCG and ECG were the relatively more abundant catechin fractions in the green tea extracts, while the other six low abundant catechins were also successfully detected as potential ligand molecules, reflecting the high sensitivity of the assay method. Interestingly, even though the caffeine had the highest signal among green tea extracts, it was not observed to form a complex with Aβ_{1-42}. Among them, EGCG was one of the most widely studied polyphenols, which was a bioactive compound derived from green tea, and currently in phase II clinical trials for AD [30]. EGCG had been reported to reduce Aβ toxicity by directly binding to Aβ monomers or by binding to oligomers/Aβ protofibrils [31,32]. In a word, forming a complex with Aβ_{1-42} was of great significance to the therapeutic function of catechins. Fortunately, the mass spectrometry signals of the complexes formed from catechins and Aβ_{1-42} had been obtained through the detection platform we built. In addition, molecules like EC-EGCG and EFG-EGCG that had not been reported to interact with Aβ_{1-42} were also screened from green tea extracts. It is worth noting that molecules with higher molecular weights may face more challenges in crossing the blood-brain barrier for AD treatment. This highlights the need for further investigation into drug delivery systems, such as nanoparticle-loaded drugs, to enhance the transport of these compounds across the barrier.

After screening the ligands, measuring the protein-ligand binding ability is also very important. Commonly used methods include isothermal titration calorimetry (ITC), fluorescence polarization immunoassay (FPIA) and surface plasmon resonance (SPR) [33,34]. However, due to the relatively small molecular weight of Aβ protein and the low binding enthalpy observed upon binding with ligands such as EGCG, we found that it was not possible to accurately measure the binding enthalpy of these small molecules directly through ITC experiments. Moreover, these methods all require pure ligand; however, some components of natural products are difficult to separate and synthesize. The mass spectrometry method can, to a certain extent, reflect the strength of the binding force through the mass spectrum signal intensity of the complex, but it will be affected by the content of the ligand in the natural product [35]. In order to avoid the tedious separation or synthesis steps of ligands and the influence of ligand content, we used MD simulation for investigating Aβ_{1-42}-ligand complex, which has been widely used to assess protein-protein/ligand interactions and properties of hits after virtual drug screening [36].

MD simulation, binding free energy and decompositions for Aβ_{1-42} and the 10 ligands had been performed. Firstly, we investigated the root mean square deviation (RMSD) of the Aβ_{1-42} backbone and small molecules within 100 ns. Taking the analysis of EC-EGCG as an example, the RMSD of the Aβ_{1-42} backbone itself and Aβ_{1-42}-EC-EGCG backbone (Fig. S4a in Supporting information) became stabilized after 55 ns, which indicated that the simulation had reached equilibrium. The 10 RMSD evolution curves indicated that each system had reached equilibrium after 80 ns (Fig. S5 in Supporting information). Then the solvent-accessibility sur-

Table 1
Ten potential ligands in green tea extracts.

Classification	Identification	Structure	Binding free energy (kcal/mol)
Catechins	EGCG	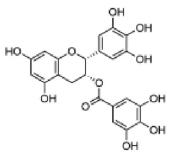	−15.01 ± 2.87
	mEGCG	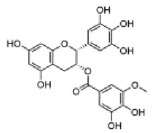	−10.49 ± 2.41
	ECG	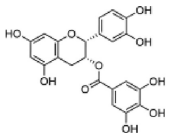	−31.97 ± 2.58
	EFG	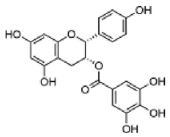	−33.21 ± 3.54
Dimers of catechins	EC-EGCG	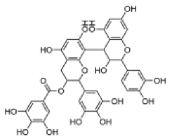	−68.54 ± 3.82
	TSA	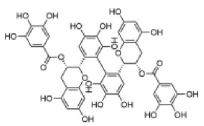	−48.85 ± 3.71
	TSF	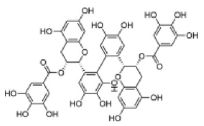	−20.17 ± 3.37
	EFG-EGCG	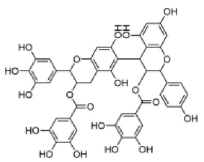	−40.24 ± 4.12
Phenolic acid	GQA	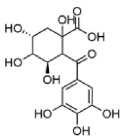	−19.2 ± 2.94
Flavonoid glucoside	VOR	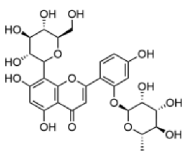	−39.29 ± 3.64

face area (SASA) of the Aβ_{1-42} in each system (Fig. S6 in Supporting information) and the number of atomic contacts (defined as the number of atomic pairs within 0.5 nm) between Aβ_{1-42} and ligands (Fig. S7 in Supporting information) were calculated to verify whether the complexes were formed between the ligands with Aβ_{1-42}. As ligand molecules approached and interacted with Aβ_{1-42}, the number of atomic contacts would increase but the SASA of Aβ_{1-42} would decrease due to the reduced exposure to solvents. It could be observed that the number of atomic contacts between Aβ_{1-42} and EC-EGCG rose greatly at 20 ns (from 500

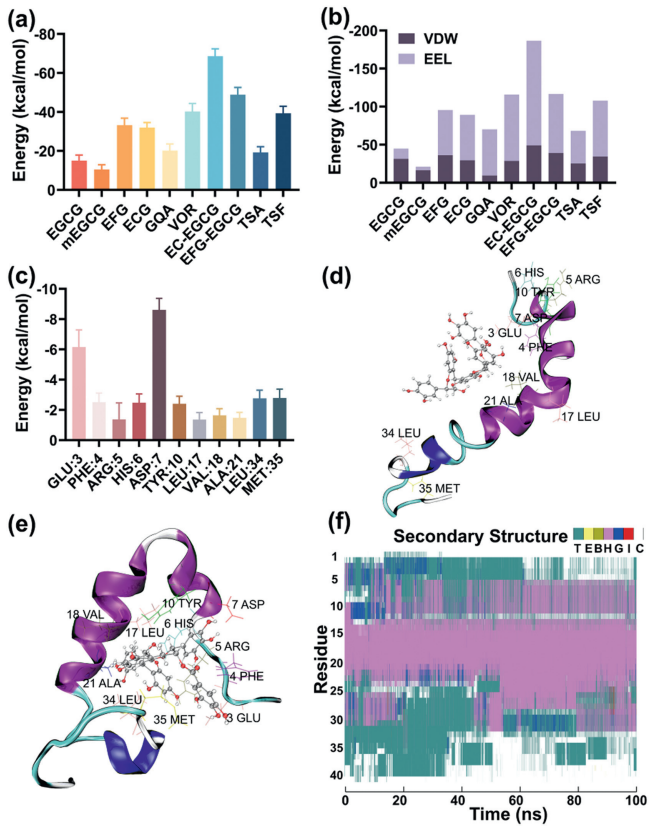

Fig. 3. MD simulation analysis of 10 complexes. (a) The binding free energy of 10 ligands. (b) The gas phase energy of ligands: van der Waals energy (VDW) and electrostatic energy (EEL). (c) The energy components (per-residue) of EC-EGCG. Data are presented as mean ± standard deviation (SD) ($n = 500$). (d) Structure of EC-EGCG molecule and Aβ_{1-42} before MD simulation taken at 0 ns. (e) A representative structure of EC-EGCG molecule bound to Aβ_{1-42} taken at 90 ns. (f) The time evolution of the secondary structures of Aβ_{1-42} in presence of EC-EGCG (T, turn; E, extended conformation; B, isolated bridge; H, alpha helix; G, 3–10 helix; I, pi-helix; C, coil).

to 1000) and 60 ns (from 1000 to 1500) (Fig. S4b in Supporting information). Meanwhile, the SASA of the protein decreased (Fig. S4c in Supporting information) thus resulting in less contact of Aβ_{1-42} with water molecules, which also could be confirmed by the reduction of the number of water molecules in the first (0–0.34 nm) and second (0.34–0.5 nm) solvation shells of Aβ_{1-42} (Fig. S4d in Supporting information). After examination of the SASA and atomic contact numbers of each system (Figs. S6 and S7), it was finally determined that all these 10 ligands could form complexes with Aβ_{1-42}.

To quantitatively compare the coordination capabilities of the ligands we screened out, we performed binding free energy calculations based on the results of MD simulations (Fig. 3a). It was worth noting that although EGCG was the most reported molecule in green tea that could form complexes with Aβ_{1-42}, 8 other molecules showed higher binding energy, and the binding free energies of EC-EGCG with Aβ_{1-42} was the highest (-68.54 ± 3.82 kcal/mol) (Table 1 for details). We further calculated the composition of gas phase energy. For EGCG and mEGCG, van der Waals forces contributed more, but for the other 8 molecules, electrostatic forces played a dominant role (Fig. 3b). Because of the lower electrostatic interaction energy, the total binding energy of EGCG and mEGCG was lower than that of the other 8 molecules. Fig. 3c showed the residues that contributed to the interactions with energy higher than -0.5 kcal/mol for EC-EFCG, from which we could see that polar residues played a major role in the binding of EC-EGCG to Aβ_{1-42}, so that electrostatic forces accounted for a greater proportion of EC-EGCG bound to Aβ_{1-42} (74% of gas phase energy). Fig. 3d and e showed the snapshot of EC-EGCG binding with Aβ_{1-42} taken at 0 and 90 ns, respectively. It was clear that EC-EGCG bound to the peptide and stayed closer to these residues. Fig. S8 (Supporting information) also showed the residues that contributed favorably to the interactions for other 9 molecules.

As a negative control, we performed 100 ns MD simulations for the interaction between caffeine and Aβ_{1-42} as well. The results of the visualization of the trajectories showed that caffeine did not interact with Aβ_{1-42}. The binding energy of caffeine and Aβ_{1-42} calculated (0.02 kcal/mol) was significantly lower than that of the 10 ligand molecules screened (Fig. S9 in Supporting information). These results showed that the strategy based on UHPLC-ESI-MS combined with MD stimulation for direct identification of NPs bound to specific protein target was an effective approach for exploring molecular interactions.

Small molecule inhibitors were reported to have an inhibitory effect on the pro-fibrillation of Aβ, as demonstrated both at the experimental level [31,32,37] and at the level of MD simulations [38,39], because of its ability to inhibit the β-sheet conformation of Aβ. Here, to further verify whether the screened ligand molecules had the potential to be inhibitors of Aβ aggregation, we performed the secondary structure analysis of each 10 complexes (Fig. S10 in Supporting information). The evolution of the secondary structures of Aβ_{1-42} presence of EC-EGCG (Fig. 3f) proved that when EC-EGCG was present, the β-sheet conformation of Aβ_{1-42} monomer could not be generated. Among other molecules we also observed an inhibitory effect on the β-sheet conformation of Aβ_{1-42} (Fig. S10), suggesting that the ligands we screened from green tea extracts had the potential to inhibit Aβ_{1-42} aggregation.

This work provided a simple but effective strategy for rapidly screening small ligand molecules from complex NPs for binding to target proteins. The on-line separation and generation of protein-ligand complexes could be achieved without the need for difficult instrumental modifications, in combination with UHPLC-ESI-MS and a peristaltic syringe pump by post-column modification technology (with a three-way valve to introduce specific protein target). Based on our designed workflow, we screened 10 bioactive components from green tea which could form complexes with Aβ_{1-42}, including EGCG and ECG that had already been widely studied, as well as EC-EGCG and EFG-EGCG that had not been reported to have the binding ability so far. The binding free energies of the ligands, as well as the decomposition energies of individual residues, were calculated by means of MD simulation, which showed that all these 10 ligands could form complexes with Aβ_{1-42}, and 8 molecules showed higher binding energy than EGCG, in which EC-EGCG demonstrated the highest binding free energy of with Aβ_{1-42} (-68.54 ± 3.82 kcal/mol). The caffeine, the highest signal among green tea extracts, was not observed to form a complex with Aβ_{1-42}, which demonstrated the selectivity and effectiveness of our strategy. Further, MD simulation's secondary structure analysis of each 10 complexes confirmed that all these 10 ligand molecules had an inhibitory effect on the β-sheet conformation of Aβ_{1-42}, which indicated the potential activity of these 10 compounds. This direct identification of NPs bound to target protein would holds promise for potentially advancing the understanding of protein-ligand interactions, facilitating drug discovery efforts, and elucidating the role of small molecules in modulating protein-protein interactions.

Declaration of competing interest

We declare that we have no known competing financial interests or personal relationships that could have appeared to influence the work reported in this paper.

CRediT authorship contribution statement

Jinqi Yang: Writing – review & editing, Writing – original draft, Methodology, Investigation, Formal analysis, Data curation, Conceptualization. **Xiaoxiang Hu:** Software. **Yuanyuan Zhang:** Methodology, Formal analysis, Data curation. **Lingyu Zhao:** Methodology, Data curation. **Chunlin Yue:** Methodology, Data curation. **Yuan Cao:** Methodology, Data curation. **Yangyang Zhang:** Writing – review & editing, Funding acquisition. **Zhenwen Zhao:** Writing – review & editing, Funding acquisition, Conceptualization.

Acknowledgment

The work was supported by the National Key R&D Program of China (No. 2018YFA0800900).

Supplementary materials

Supplementary material associated with this article can be found, in the online version, at doi:10.1016/j.cclet.2024.110128.

References

[1] P. Gao, J. Chen, P. Sun, et al., Chin. Chem. Lett. 34 (2023) 108296.
[2] X. Wu, X. Chen, X. Wang, et al., Chin. Chem. Lett. 35 (2024) 108756.
[3] B. Zhang, S. Zhao, D. Yang, et al., ACS Cent. Sci. 6 (2020) 213–225.
[4] D.J. Newman, Natl. Sci. Rev. 9 (2022) nwac206.
[5] T. Pluskal, J.K. Weng, Chem. Soc. Rev. 47 (2018) 1592–1637.
[6] T.N. O'Connell, J. Ramsay, S.F. Rieth, et al., Anal. Chem. 86 (2014) 7413–7420.
[7] Y. Lu, S. Qin, B. Zhang, et al., Anal. Chem. 91 (2019) 8162–8169.
[8] Z. Wang, H. Liang, H. Cao, et al., Analyst 144 (2019) 2881–2890.
[9] G.T.H. Nguyen, J.L. Bennett, S. Liu, et al., J. Am. Chem. Soc. 143 (2021) 21379–21387.
[10] S. Tamara, M.A. den Boer, A.J.R. Heck, Chem. Rev. 122 (2022) 7269–7326.
[11] A. Chowdhury, J. Sarkar, T. Chakraborti, et al., Biomed. Pharmacother. 78 (2016) 50–59.
[12] S. Zhang, Q. Zhu, J.-Y. Chen, et al., Phytomedicine 79 (2020) 153316.
[13] N. López-Gutiérrez, R. Romero-González, P. Plaza-Bolaños, et al., Food Chem. 173 (2015) 607–618.
[14] Z. Xin, S. Ma, D. Ren, et al., Food Chem. 266 (2018) 534–544.
[15] B. Han, Z. Xin, S. Ma, et al., J. Chromatogr. B 1063 (2017) 84–92.
[16] M. Bedner, D.L. Duewer, Anal. Chem. 83 (2011) 6169–6176.
[17] L. Ridder, J.J.J. van der Hooft, S. Verhoeven, et al., Anal. Chem. 85 (2013) 6033–6040.
[18] N. Kuhnert, J.W. Drynan, J. Obuchowicz, et al., Rapid Commun. Mass Spectrom. 24 (2010) 3387–3404.
[19] J. Choi, E.M. Kim, B.J. Ko, et al., Biotechnol. Bioprocess Eng. 27 (2022) 253–261.
[20] F.M. LaFerla, K.N. Green, S. Oddo, Nat. Rev. Neurosci. 8 (2007) 499–509.
[21] D.J. Selkoe, Nat. Cell Biol. 6 (2004) 1054–1061.
[22] S.I.A. Cohen, S. Linse, L.M. Luheshi, et al., Proc. Natl. Acad. Sci. U. S. A. 110 (2013) 9758–9763.
[23] P.H. Nguyen, A. Ramamoorthy, B.R. Sahoo, et al., Chem. Rev. 121 (2021) 2545–2647.
[24] J. Sevigny, P. Chiao, T. Bussière, et al., Nature 537 (2016) 50–56.
[25] J. Hu, Y. Zhao, Y. Li, Chin. Chem. Lett. 34 (2023) 107623.
[26] Y. Jiang, Z. Zeng, J. Yao, et al., Chin. Chem. Lett. 34 (2023) 107966.
[27] H. Zeng, Y. Qi, Z. Zhang, et al., Chin. Chem. Lett. 32 (2021) 1857–1868.
[28] K.P. Kepp, Chem. Rev. 112 (2012) 5193–5239.
[29] L.M. Young, J.C. Saunders, R.A. Mahood, et al., Nat. Chem. 7 (2015) 73–81.
[30] F.-F. Liu, X.-Y. Dong, L. He, et al., J. Phys. Chem. B 115 (2011) 11879–11887.
[31] D.E. Ehrnhoefer, J. Bieschke, A. Boeddrich, et al., Nat. Struct. Mol. Biol. 15 (2008) 558–566.
[32] J. Bieschke, J. Russ, R.P. Friedrich, et al., Proc. Nat. Acad. Sci. U. S. A. 107 (2010) 7710–7715.
[33] Z. Chen, Y. Shi, F. Zhong, et al., Chin. Chem. Lett. 36 (2025) 109956.
[34] D. Liu, S. Liu, F. Hu, et al., Chin. Chem. Lett. 35 (2024) 108762.
[35] J.L. Bennett, G.T.H. Nguyen, W.A. Donald, Chem. Rev. 122 (2022) 7327–7385.
[36] T. Róg, M. Girych, A. Bunker, Pharmaceuticals 14 (2021) 1062.
[37] X.R. Cheng, B.Y.H. Hau, A.J. Veloso, et al., Anal. Chem. 85 (2013) 2049–2055.
[38] X. Dong, Y. Tang, C. Zhan, et al., Chem. Phys. Lipids 234 (2021) 105024.
[39] R. Ahmed, B. VanSchouwen, N. Jafari, et al., J. Am. Chem. Soc. 139 (2017) 13720–13734.